Structure and Electronic Properties of MoS_2 Nanotubes

Gotthard Seifert,[1] Humberto Terrones,[2,3,*] Mauricio Terrones,[3,4] Gerd Jungnickel,[1] and Thomas Frauenheim[1]
[1]*Theoretische Physik, Universität-GH Paderborn, 33098 Paderborn, Germany*
[2]*School of Chemistry, Physics and Environmental Science, University of Sussex, Brighton, BN1 9 QJ, United Kingdom*
[3]*Instituto de Física, UNAM, Laboratorio Juriquilla, Apartado Postal 1-1010, 76000 Querétaro, México*
[4]*Max Planck Institut für Metallforschung, Seestrasse 92, Stuttgart D-70174, Germany*

(Received 4 November 1999)

Structural and electronic properties as well as the stability of MoS_2 nanotubes are studied using the density-functional-based tight-binding method. It is found that MoS_2 zigzag $(n, 0)$ nanotubes exhibit a narrow direct band gap and MoS_2 armchair (n, n) possess a nonzero moderate direct gap. Interestingly, the (n, n) tubes show a small indirect gap similar to the direct gap of $(n, 0)$ nanotubes. Simulated electron diffraction patterns confirm the existence of armchair and zigzag disulphide nanotubes. The structure of the MoS_2 nanotube tips is explained by introducing topological defects which produce positive and negative curvature.

PACS numbers: 71.20.Tx, 61.48.+c

The discoveries of fullerenes and carbon nanotubes [1,2] as new forms of matter in the nanoscale range have opened a challenging new field in solid state physics, chemistry, and materials science with a wide spectra of possible applications. Boron nitride (BN) nanotubes and nanoparticles have also been synthesized and their properties are still under investigation [3]. Moreover, Tenne *et al.* have successfully produced inorganic fullerenelike and tubular structures from more complex layered compounds such as tungsten disulphide (WS_2) and molybdenum disulphide (MoS_2) [4,5]. It has been shown that polyhedral particles of MoS_2 and WS_2 behave as exceptional lubricants [6]. Recently, it was found that WS_2 nanotube tips improve image quality in scanning probe microscopy [7]. Nevertheless, electronic and mechanical properties of metal disulphide nanotubes have not yet been reported hitherto. In this Letter we address, for the first time, the problem of the stability and electronic properties of zigzag and armchair MoS_2 nanotubes using the density-functional-based tight-binding (DFTB) method [8]. Our results demonstrate that the strain energy of all the nanotubes (both zigzag and armchair) behaves similarly to carbon nanotubes [9]. We predict that all MoS_2 nanotubes observed (>20 Å outside diameter) should be semiconductors with a band gap smaller than bulk MoS_2, which size depends upon diameter and chirality. Our simulated diffraction patterns of disulphide nanotubes coincide with those reported experimentally, thus confirming the existence of armchair and zigzag tubules. Furthermore, we propose topological defects which explain the structure of MoS_2 nanotube tips and the closure of polyhedral particles.

The most stable form of layered MoS_2, as well as WS_2, consists of a metal layer sandwiched between two sulphur layers (space group $P63/mmc$). These triple layers are stacked together, similarily to graphite, by van der Waals interactions separated 6.15 Å for MoS_2 and 6.18 Å for WS_2. Therefore, tubular structures can be analogously constructed by conformal mapping of a 2D triple layer of MoS_2 onto the surface of a cylinder, thus rolling up the sheets along specific directions in the 2D lattice (see Fig. 1). As for the carbon nanotubes [2] this may be described in terms of the primitive 2D lattice vectors $\vec{a}$ and $\vec{b}$ and two integer indices [10]: $\vec{B} = n\vec{a} + m\vec{b}$. In this way three classes of nanotubes can be distinguished: $n = m$ "armchair" nanotubes, $n \neq 0, m = 0$ "zigzag" nanotubes, and $n \neq m$ "chiral nanotubes." Therefore, these nanotubes are composed of a triple layer of atoms with a finite "wall

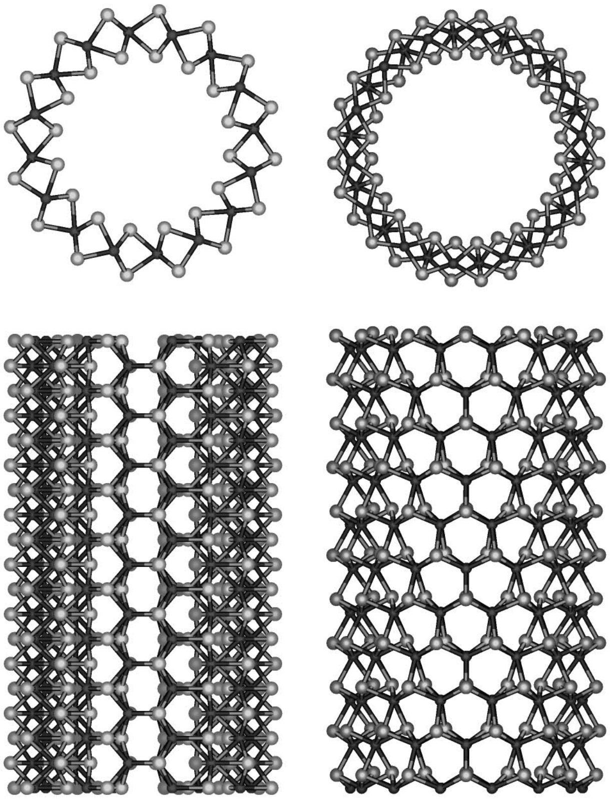

FIG. 1. Armchair (8,8) MoS_2 nanotube (left) and zigzag (14,0) MoS_2 nanotube (right). Light atoms are S; dark atoms are Mo.

thickness" exhibiting certain "roughness" on the outer shell (see Fig. 1).

Our calculations [8] were performed for (n,n) and $(n,0)$ MoS_2 nanotubes as a function of n with diameter (D) ranging between 8 and 26 Å, which correspond to indices $(n,0)$-(n,n) from $(10,0)$-$(6,6)$ to $(22,0)$-$(14,14)$, respectively. The largest diameters are in agreement with the smallest experimentally observed tubes [4,5]. The optimized bond lengths for the tubes are slightly larger than those of the planar sheet. The Mo-S bond length within the inner shell is increased only by approximately 0.01 Å and the Mo-S bond length on the outer shell increases by 0.04 Å. The Mo-Mo distance is greater than that of the flat sheet by nearly 0.25 Å. The calculated strain energies follow roughly a $1/D^2$ behavior as in carbon nanotubes [9]—see Fig. 2a. However, the strain energy for the smallest MoS_2 tubes is at least 1 order of magnitude larger than that of carbon nanotubes (NTs) with similar diameter. This result is not surprising, since the rolling of a triple layer into a narrow tube causes much more energy penalty than rolling a monolayer. But at about 20 Å tube diameter, the strain energy is now lowered to reasonable values, as known for carbon nanotubes [9], which fit to the experimental observation for the narrower MoS_2 nanotubes. The strain energies for armchair (n,n) MoS_2 nanotubes are slightly more favorable than for zigzag $(n,0)$ at a given diameter (see Fig. 2a).

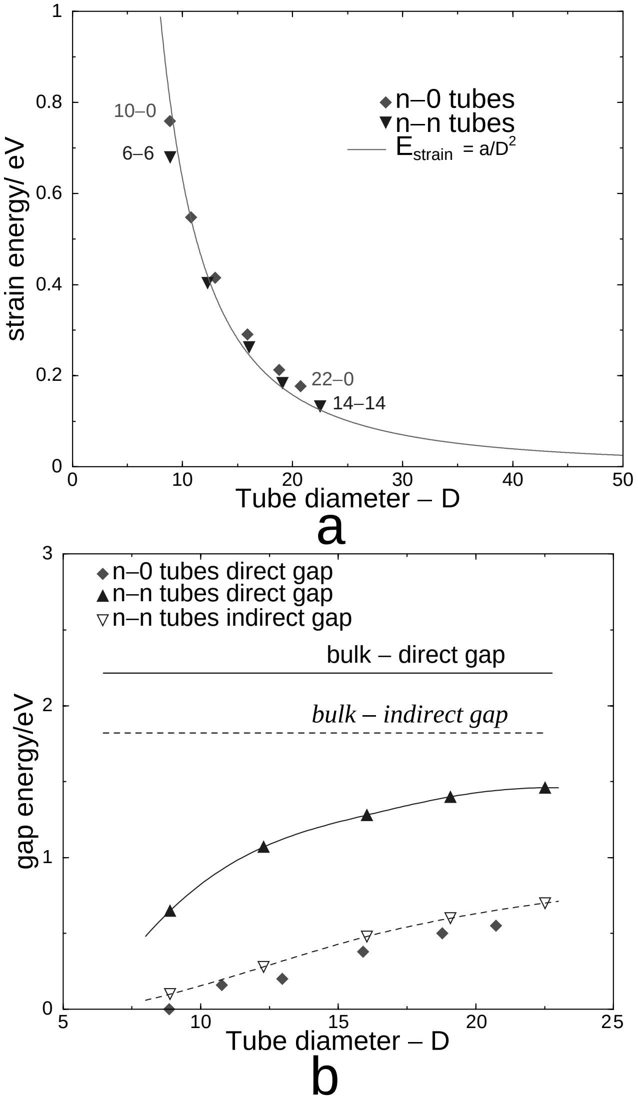

FIG. 2. (a) Calculated strain energies of MoS_2 nanotubes (energy per atom relative to the infinite single MoS_2 triple layer) as a function of tube diameter in Å. (b) Calculated gap energies of MoS_2 nanotubes as a function of tube diameter in Å.

The charge transfer from molybdenum $(Q = +0.9)$ to sulphur $(Q \approx -0.44$ each S) within the tubes is nearly the same as in the MoS_2 triple layer, and there is only a minor difference between outer and inner sulphurs. The main features of the calculated density-of-states (DOS) curves (not shown here) are quite similar for all tubes and also similar to that of the planar triple layer. The DOS is characterized by a well separated peak corresponding to a sulphur s band of about 2 eV width and 14 eV below the valence band edge. This is followed, at higher energy, by the valence bands with a width of about 7 eV, formed by hybridized Mo d and sulphur p states. The corresponding antibonding states characterize the conduction band. The Mo d states especially dominate the upper valence band edge as well as the lower conduction band edge. These features are in agreement with results from band structure calculations for bulk MoS_2 [11–13].

Figure 3a shows the band structure around the Fermi energy of a single-sandwich MoS_2 characterizing this layer, as well as the bulk material, as a semiconductor. The single-sandwich (triple layer) has an indirect gap $(\Gamma \rightarrow K)$ and a direct gap at the K point. The calculated band structure agrees also qualitatively well with calculations reported by other groups [12,14]—see Fig. 3a.

The band structure of the MoS_2 NTs can be derived formally from the layer band structure [10]. The band structure of the $(n,0)$ MoS_2 NTs resemble that of the corresponding carbon NTs; however, in contrast to carbon NTs, the gap size increases with increasing tube diameter, but still being smaller than the gap for a single triple layer and the bulk material in the size region considered here (see Figs. 2b and 3). Similar behavior has been reported theoretically for GaSe nanotubes [15]. However, our results are fully consistent with experimental observations of the optical-absorption spectra of MoS_2 nanotubes and inorganic fullerenelike structures [14].

The gap size of zigzag nanotubes is intimately related to that at the K point in the MoS_2 layer. Since MoS_2 layers exhibit a finite gap at the K point (see Fig. 3a), zigzag NTs are not expected to have a vanishing gap at certain n. In fact, we have not found $(3n,0)$ "irregularities" in gap size, as they were proposed for carbon. i.e., none of the "zigzag" MoS_2 NTs will be metallic. Furthermore, while the (n,n) carbon NTs are all metallic, the (n,n) MoS_2 NTs behave differently: they all have a nonzero direct gap

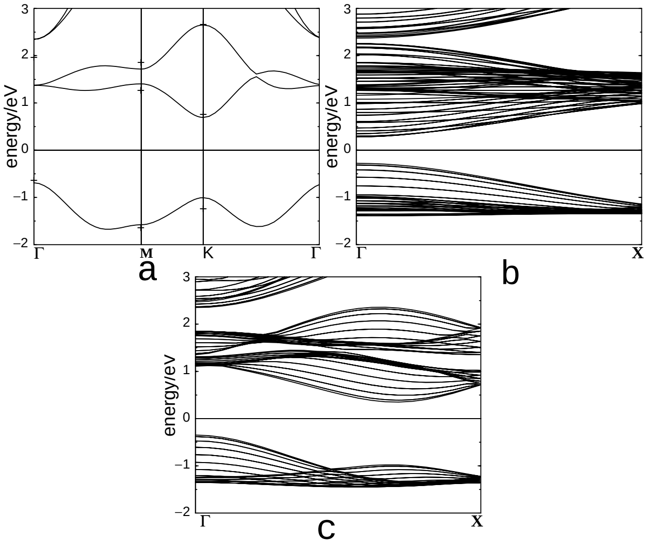

FIG. 3. (a) Calculated band structure near the Fermi energy (E_F) for a MoS_2 single-sandwich (“triple layer”). The energy is given relative to E_F. Band energies at several K points, indicated by +, from band structure calculations by Kobayashi and Yamauchi [12] are given for comparison. (b) Calculated band structure for a MoS_2 (22,0) nanotube. (c) Calculated band structure for a MoS_2 (14,14) nanotube.

and indirect gaps down to the smallest tubes (see Fig. 3c), which increase smoothly with increasing diameter. The size of the indirect gaps for the (n, n) tubes is close to that of the direct gaps of the $(n, 0)$ tubes with similar diameter (see Fig. 2b).

Electron diffraction is a very useful technique for characterizing structural features caused by different chiral arrangements in NTs. We have calculated diffraction patterns for MoS_2 and WS_2 NTs showing that there are planes which can be identified with the 110 (1.58 Å for MoS_2 and 1.577 Å for WS_2) and the 100 (2.737 Å for MoS_2 and 2.731 Å for WS_2) of crystalline MoS_2 and WS_2 obtained when the beam is perpendicular to the sheets (see Fig. 4). In the same patterns, due to the curvature of the cylinders and thickness, there are characteristic reflections which are in agreement with plane distances observed in MoS_2 (and WS_2) crystals when the flat layers are parallel to the electron beam. The 002 reflections are not present because we are only considering cylinders with one single (triple) layer of MoS_2, not multiwalled. In other words, since the MoS_2 NTs are closed curved sheets with certain thickness, their diffraction exhibits the superposition of reflections associated with different orientations of the infinite flat crystal. The finite dimensions of the tubes in the direction perpendicular to the tube axis (tube diameter) and the periodic order along the axis (direction of growth) produce diffraction spots elongated perpendicularly to the axis. Tenne *et al.* have shown experimental electron diffraction of MoS_2 and WS_2 NTs which corresponds to our armchair and zigzag simulated patterns [4,16], proving the existence of these types of NTs. Although we have not considered chiral NTs, electron diffraction evidence suggests that these also exist [16].

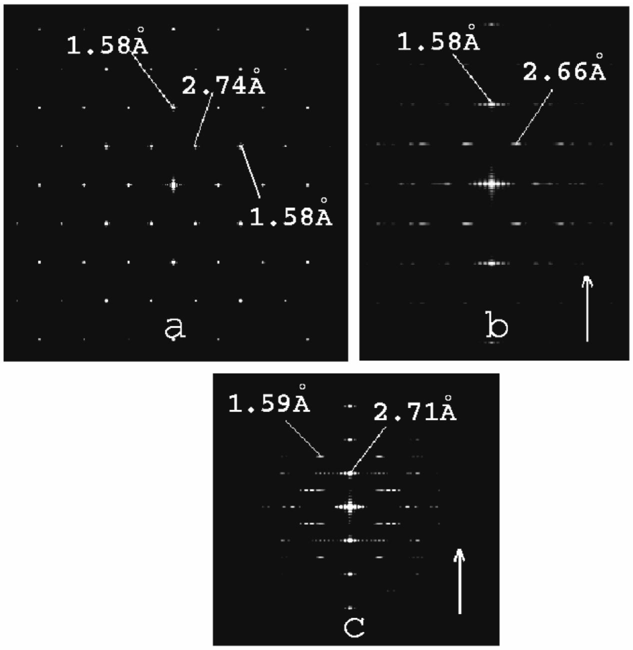

FIG. 4. Simulated electron diffraction patterns showing similar distance planes for (a) flat triple MoS_2 layer. (b) Armchair (14,14) MoS_2 nanotube. (c) Zigzag (22,0) MoS_2 nanotube (the arrows show the direction of the tube axis).

In order to explain the observed MoS_2 NTs tips [4] and the structure of the MoS_2 and WS_2 polyhedral particles [17], we have introduced topological defects which can preserve the stoichiometry of the system and can produce positive and negative Gaussian curvatures. One possibility is to close zigzag nanotubes with three squarelike defects (SQDs) as shown in Figs. 5a and 5c. Armchair nanotubes can be closed using four SQDs and one octagonal-like defect (OLD) (see Figs. 5b and 5d). The OLD introduces negative curvature into the system which is balanced by the addition of one SQD (positive curvature) satisfying Euler’s law analogously as in graphite. Similar closed BN structures, first proposed by Terrones *et al.* [3], have also been theoretically confirmed [18]. Regarding the presence of OLD defects, it is worth mentioning that negative curvature in disulphide structures has been reported by Tenne’s group [5].

In summary, MoS_2 NTs are stable with strain energies decreasing as the diameter grows; in this respect they are similar to carbon nanotubes. However, electronically they behave differently since MoS_2 NTs are not metallic, being all semiconducting. We observe two types of narrow band gap NTs: the (n, n) tubes exhibiting a small indirect and a moderate direct gap, and the $(n, 0)$ possessing a small direct gap: this suggests that zigzag NTs can be used for optoelectronics, i.e., luminescing devices, which is not possible with carbon NTs. Because of the structural similarities between MoS_2 and WS_2 layers, we expect similar

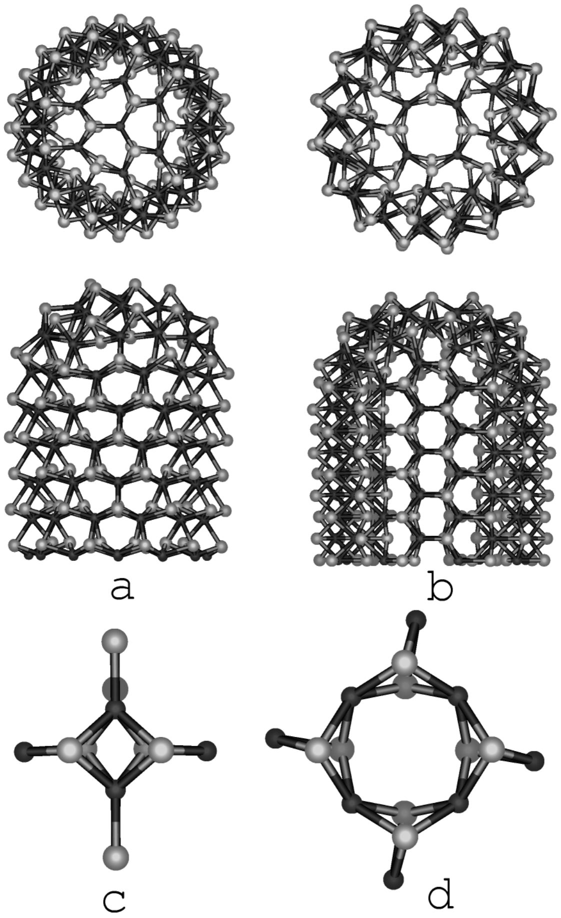

FIG. 5. MoS_2 nanotube tips (a) zigzag (12,0) tube closed with three squarelike defects. (b) Armchair (8,8) tube closed with four squarelike defects and one octagonal-like defect. (c) Squarelike defect. (d) Octagonal-like defect.

electronic and mechanical behavior. We have considered the most stable phase of MoS_2; however, metastable phases such as the octahedral reported by Yang *et al.* [19] (also layered) might have different electronic behavior shifting the Fermi energy into a Mo d band possibly leading to metallic NTs. Another possible way to shift E_F could be the replacement of Mo by Nb.

The defects that we have used to close the NTs might shed some light in explaining the different topologies observed as well as the electronic and mechanical properties of the MoS_2 NTs tips and inorganic fullerenes.

Graphite, boron nitride, MoS_2, and WS_2 are the first examples of layered materials that can generate curved structures such as fullerenes, polyhedral particles, and nanotubes. Therefore, further theoretical and experimental investigations on layered compounds promise a fertile ground for fascinating curved nanomaterials with remarkable properties.

We thank D. R. M. Walton, H. W. Kroto, and E. Hernández for fruitful discussions. G. S. thanks F. Seifert for his computational assistance. We are grateful to the Sächsische Ministerium für Wissenschaft und Kunst (G. S.), the Royal Society (M. T., H. T.), CONACYT-México 25237-E (H. T.), and J31192U (M. T., H. T.), DGAPA-UNAM sabbatical scheme and Grants No. 108-199, IN119-698 (H. T.), and The Alexander von Humboldt–Stiftung (M. T.) for financial assistance.

---

*Corresponding author.

[1] H. W. Kroto *et al.*, Nature (London) **318**, 162 (1985).
[2] S. Iijima, Nature (London) **354**, 56 (1991).
[3] N. G. Chopra *et al.*, Science **269**, 966 (1995); A. Loisseau *et al.*, Phys. Rev. Lett. **76**, 4737 (1996); M. Terrones *et al.*, Chem. Phys. Lett. **259**, 568 (1996); D. Golberg *et al.*, Appl. Phys. Lett. **69**, 2045 (1996).
[4] R. Tenne *et al.*, Nature (London) **360**, 444 (1992); L. Margulis *et al.*, Nature (London) **365**, 113 (1993).
[5] R. Tenne, M. Homyonfer, and Y. Feldman, Chem. Mater. **10**, 3225 (1998).
[6] L. Rapoport *et al.*, Nature (London) **387**, 791 (1997).
[7] A. Rothschild, S. R. Cohen, and R. Tenne, Appl. Phys. Lett. **75**, 4025 (1999).
[8] D. Porezag *et al.*, Phys. Rev. B **51**, 12 947 (1995); G. Seifert, D. Porezag, and Th. Frauenheim, Int. J. Quantum Chem. **58**, 185 (1996). The repulsive potential in the DFTB treatment was obtained by fitting DFT energies for the corresponding dimers (Mo-Mo, Mo-S, S-S) as reference systems. This treatment gives DFTB optimized bond lengths for MoS_2 triple layers within an accuracy of 2%, compared to experimental data for bulk MoS_2.
[9] E. Hernández *et al.*, Phys. Rev. Lett. **80**, 4502 (1998).
[10] N. Hamada, S. Sawada, and A. Oshiyama, Phys. Rev. Lett. **68**, 1579 (1992).
[11] R. Coehoorn *et al.*, Phys. Rev. B **35**, 6195 (1987).
[12] K. Kobayashi and J. Yamauchi, Phys. Rev. B **51**, 17 085 (1995).
[13] J. D. Fuhr, J. O. Sofo, and A. Saul, Phys. Rev. B **60**, 8343 (1999).
[14] G. L. Frey *et al.*, Phys. Rev. B **57**, 6666 (1998); G. L. Frey *et al.*, J. Mater. Res. **13**, 2412 (1998).
[15] M. Coté, M. L. Cohen, and D. J. Chadi, Phys. Rev. B **58**, R4277 (1998).
[16] L. Margulis *et al.*, J. Microsc. **181**, 68 (1996).
[17] P. A. Parilla, A. C. Dillon, K. M. Jones, G. Riker, D. L. Schulz, D. S. Ginley, and M. J. Heben, Nature (London) **397**, 114 (1999).
[18] X. Blase, A. De Vita, J. C. Charlier, and R. Car, Phys. Rev. Lett. **80**, 1666 (1998); S. S. Alexandre, M. S. C. Mazzoni, and H. Chacham, Appl. Phys. Lett. **75**, 61 (1999).
[19] D. Yang *et al.*, Phys. Rev. B **43**, 12 053 (1991).